Thermal evaluation of a highly insulated steel stud wall with vacuum insulation panels using a guarded hot box apparatus

Moore, Travis V.; Cruickshank, Cynthia A.; Beausoleil-Morrison, Ian; Lacasse, Michael

Publisher’s version / Version de l'éditeur:
https://doi.org/10.1177/1744259120980030
Journal of Building Physics, pp. 1-20, 2020-12-27

Thermal evaluation of a highly insulated steel stud wall with vacuum insulation panels using a guarded hot box apparatus

Travis V. Moore[a,b,]*, Cynthia A. Cruickshank[b], Ian Beausoleil-Morrison[b], Michael Lacasse[a]

[a] *National Research Council Canada, 1200 Montreal Road, Ottawa, Ontario, Canada, K1A0R6*

[b] *Carleton University, 1125 Colonel By Drive, Ottawa, Ontario, Canada, K1S 5B6*

* *Corresponding author: Travis.Moore@nrc-cnrc.gc.ca, +1 613-949-0194*

Abstract

This paper presents the results of a Guarded Hot Box (GHB) experiment on a wall assembly made up of both steel stud framing and an external insulating assembly which incorporates vacuum insulation panels (VIPs) for which knowledge of the composition of the VIP barrier foil is not readily available. The purpose of the tests is to provide an experiment result for thermal resistance of a wall assembly containing several sources of thermal bridging, including those due to the barrier foil at the edge of and joint material between the VIPs and the condensation potential on the interior surface due to the steel studs.

The steady-state GHB experiments were completed in accordance with ASTM C1363 for an interior air temperature of 20.9°C and an exterior air temperature of -34.9°C; this resulted in a thermal resistance for the wall assembly of 6.8 ± 0.8 m^2K/W. Surface temperature measurements on a VIP in the wall assembly indicated that increased levels of heat transfer were occurring at the edges of the VIPs as compared to the centre of the panel confirming thermal bridges were present at the panel edge. Measurement of the temperature on the interior surface of the sheathing board around the steel stud indicated that the external insulation effectively minimized the risk of condensation due to the steel studs.

Determining the thermal resistance and condensation risk for a wall assembly which contains VIPs for which knowledge of the barrier film is not readily available demonstrates the potential for use

of such a wall assembly according to energy and building code requirements. The wall assembly and test details can also be used to compare industry standard calculation methods and detailed 2D and 3D simulations to the GHB test result. The comparison can be used to inform on the validity of using calculations and simulation methods in lieu of testing for energy and building code compliance. The comparison of calculations and simulations is not the scope of the work presented in this paper and will be explored in future publications.

Keywords: Guarded hot box, Vacuum insulation panels (VIP), Thermal bridges, Steel Stud

Funding: This work was supported by the Construction Research Centre of the National Research Council of Canada; however, this research did not receive any specific grant from funding agencies in the public, commercial, or not-for-profit sectors.

Introduction

Building on the Paris Agreement (United Nations, 2015), many countries have developed plans to combat climate change by reducing GHG emissions in an effort to contribute to the goal of limiting global temperature increase to well below 2°C. The Government of Canada, through the Pan-Canadian Framework on Clean Growth and Climate Change (Government of Canada, 2018), has set a target of reducing the GHG emissions to 30% below 2005 levels. Of Canada's total GHG emissions 17% is associated with homes and buildings, made up of 12% from direct emissions (e.g., combustion of natural gas for heating) and 5% from emissions associated with electricity generation consumed in the built environment (Government of Canada, 2018). Therefore, reducing the heating and cooling loads in buildings has been identified as a significant contributor towards the 2030 GHG reduction goal. The most direct method for this to occur in Canada is to decrease the minimum energy performance required of buildings in the National Model Codes – specifically the National Energy Code of Canada (National Research Council Canada, 2016) and the

National Building Code of Canada (National Research Council Canada, 2015). The direct method these codes have implemented to reduce building GHGs is to increase the minimum effective thermal resistance (including thermal bridge effects) requirements of walls and roofs.

North American Energy codes, such as the National Energy Code of Canada for Buildings (NECCB) (National Research Council Canada, 2016) and ASHRAE 90.1 (ASHRAE, 2016), reference several methods to determine the thermal resistance of a wall assembly including both experimental and calculation methods (ISO 10211-07, 2007; ISO 6946-07, 2007; ISO 14683-07, 2007). Although accounting for thermal bridges is mentioned in the energy codes, the methods referenced typically deal with large thermal bridges such as parapets, balconies, or slab edges. Little information is provided to calculate the effect of thermal bridges for individual components in wall assemblies other than framing components, such as steel and wood studs (National Research Council Canada, 2016; ASHRAE, 2016; ASHRAE, 2016). The necessity in accounting for thermal bridges in determining the thermal performance of building envelopes is well understood; ignoring lateral heat transfer from larger structural components (balconies, slab edges, parapets, etc.) has been documented to result in a potential underestimate of the heat transmission by 20% to 70% (Morris and Hershfield, 2014) (ASHRAE, 2011). The typical method of accounting for the thermal bridging effects of these larger components is through the linear transmittance method (ISO 14683-07, 2007). For smaller repeating thermal bridge elements, such as steel and wood framing, there are specific calculation methods that are used to define the thermal bridge heat transfer effects that have been investigated.

The need for methods to deal with thermal bridges other than structural components becomes particularly important in wall assemblies with high thermal resistance, especially when the high thermal resistance is due to the presence of vacuum insulation panels (VIPs). This is due to the high degree of thermal bridging that occurs over the edge of the panel due to the barrier foil and the joint material between panels. A VIP is made up of two main components: the core material and the gas barrier film. The VIP core is made up of a material that is open cell, microporous, with a fractal composition and compressive strength high enough to maintain its shape when under partial vacuum (~1 mbar) (Simmler, et al., 2005; Schwab, Stark, Wachtel, Ebert, & Fricke, 2005). However, to maintain the partial vacuum in the core material, a gas barrier film is required to limit the migration of atmospheric gases and water vapour to the core material. Unfortunately, currently the best materials for reduction of gas and vapour transmission are metals which decreases the thermal performance of the VIP as it acts as a thermal bridge. Due to the VIP deriving a significant portion of its thermal resistance from the partial vacuum of the pores in the core material, the gas barrier film obviously cannot be perforated. This necessitates a combination of panels required for wall construction, to allow for cladding fasteners, duct and pipe penetrations etc. The assembly of multiple panels causes a second thermal bridge through the joints between panels, as the material in the joints has a higher thermal transmittance than the centre of the VIP panel. Biswas et al. (Biswas, et al., 2018) describe development of an alternative technology of vacuum insulation technology made of composite foam insulation boards coupled with vacuum insulated cores, that can be cut and penetrated and remain effective, however this technology is still in development.

The effects of thermal bridging in VIPs has been well explored in several publications, a selection of which are described here. Ghazi Wakili et al. (Ghazi Wakili & Nussbaumer, 2005) determined the linear thermal transmittance and total heat loss for 20mm and 30mm thick VIPs of 1300 mm in width by 600 mm in height. The work reduced the multilayer barrier film to a single layer and assumed a centre of panel thermal conductivity of 0.008 W/mK. The results of the work across different building envelope scenarios showed that the edge effect of the VIP is also dependent on the material used surrounding the VIP, and therefore need to be calculated per case, not simply for the VIP in isolation. Schwab et al. (Schwab, Stark, Wachtel, Ebert, & Fricke, 2005) used numerical simulations to investigate the effect of different barrier foil compositions and gaps on the linear thermal transmittance of the panels. Tenperik & Cauberg (Tenperik & Cauberg, 2007) developed a method to analytically calculate the corresponding edge thermal transmittance of VIPs accounting for: the heat transmission coefficient at the boundary surface, the thickness of the VIP, the thickness of the laminate, the thickness of the laminate at the panel edge and the thermal conductivity of the laminate. Van Den Bossche et al. (Van Den Bossche, Moens, Janssens, & Delvoye, 2010) compared the analytical method proposed by Tenpirek to experimental results. The experimental work included isolating the effect of the barrier film and air gap separately. Comparison of the experiment results to Tenperik's analytical method determined that the equations overestimated the thermal transmittance of the edge values by approximately 8% for a 20mm thick panel and 23% for a 30mm thick panel. Sprengard and Holm (Sprengard & Holm, 2014) investigated the thermal losses on the edge of panels through numerical simulations, accounting for influences of: thickness of the panels, type of edge design (single or multiplayer foils), inorganic barrier material and thickness of barrier layers, the material used between the joints, fasteners used to mount the panels, as well as encasement material. Lorenzati et al. (Lorenzati, Fantucci, Capozzoli, & Perino, 2014) evaluated 20 mm thick VIPs with three different metallized barriers and four different materials in the joint between abutting VIPs. The joints evaluated included air, XPS (extruded polystyrene), MDF (medium density fibreboard) and rubber. The linear thermal transmittance of the edge and joints for each case were determined using a heat flow meter apparatus. For application to various VIP sizes and air gap widths, the results were normalized by perimeter to area ratio.

The performance of VIPs has also been investigated in guarded hot box tests. Nussbaumer (Nussbaumer, Bundi, & Muehlebach, 2005) completed an experimental and numerical evaluation of a wooden leaf door containing VIPs and additionally characterized the performance of damaged VIPs; for the whole door system a single damaged VIP reduced the performance by 8.5% and 14% for two damaged panels. Nussbaumer (Nussbaumer, Ghazi Wakili, & Tanner, 2006) also investigated the thermal performance of a concrete wall externally insulated with six expanded polystyrene boards which contained three VIPs using a GHB and numerical simulations for both intact and damaged VIPs; the consequences of a VIP losing its vacuum was determined change the effective thermal conductivity from 0.0053 to 0.020 W/mK.

Methods to evaluate the in-situ performance of wall systems containing steel studs and/or VIPs have also been investigated. Mandilaras et al. (Mandilaras, Atsonios, Zannis, & Founti, 2014) investigated the in-situ performance of a full scale wall with conventional ETICs using EPS (expanded polystyrene) for 2 years, thereafter replacing the EPS in the north facing wall with VIPs. The results indicated that the VIP outperformed the EPS, however performed 27% less than the theoretical estimates. Atsoniois (Atsonios, Mandilaras, Kontogeorges, & Founti, 2018) investigated two methods to determine the in-situ thermal transmittance of cold frame lightweight steel stud walls, consisting of the Representative Points Method and Weighted Area Method. They determined that methods using a thermal camera could be used for in-situ evaluations, however the temperature difference between the interior surface at the steel stud and the unaffected areas needed to be a minimum of 0.7°C. Atsonios et al. (Atsonios, Mandilaras, Manolitsis, Kontogeorgos, & Founti, 2007) investigated the in-situ performance of a building which had lightweight steel studs and VIPs. The experiments were used to validate a whole building energy performance model which was used in a parametric study of different climate locations (Athens, Oslo, New York, Kuwait) resulting in an average energy savings of 19%. Kontogeorgos et al. (Kontogeorgos, Atsonios, & Mandilaras, 2016) investigated the in-situ performance of a two storey structure containing lightweight steel studs and VIPs finding that the VIPs decrease the total thermal transmittance of the structure by approximately 33%.

The literature reviewed indicates that VIPs have significant potential to be used to increase the thermal resistance of a wall assembly in both new and retrofit scenarios. The review also indicates the thermal performance of a VIP wall system cannot be properly calculated unless the thermal bridges around the panel edges and joints are accounted for. Calculating the effective thermal conductivity of a VIP to a reasonable degree is possible if knowledge of the barrier film composition is available. Otherwise, experiments must be completed to characterize the thermal performance of a wall system incorporating VIPs. From the literature review the tests completed that account for wall assemblies containing both VIP and steel studs were completed on in-situ experiments rather than a wall assembly in a GHB. Determining the thermal resistance and potential for condensation of a generic wall assembly incorporating VIPs and steel studs in a GHB demonstrates the potential for use of such a wall assembly according to energy and building code requirements. Additionally, geometry descriptions of the wall assembly and controlled boundary conditions of the GHB enable comparison to industry standard calculation methods and detailed 2D and 3D simulations.

As such, the purpose of this paper is to detail the results of a GHB test, including descriptions of the wall geometry and boundary conditions during the test, for a representative highly insulated commercial type wall assembly containing both vacuum insulated panels (VIP) and steel studs for which the exact composition of the barrier film is not readily available. Comparison of the results to calculation and simulation methods is not in the scope of this paper and will be described in future work. This wall contains several sources of thermal bridging, including: the barrier foil surrounding the VIP panel, the joint material between the VIPs (air), fiberglass clips for the exterior insulation layer, the steel studs and fasteners. Instrumentation is installed to determine the temperature difference between the center and edge of a VIP, as well as the effect of the steel stud on the interior sheathing board surface temperature. The GHB test apparatus is characterized in accordance with ASTM C1363. This paper describes the construction details of the wall assembly, the instrumentation locations during the experiments, the experiment apparatus, the uncertainty of the experiment, and the experiment results.

Experiment method and wall assembly

Guarded hot box

The steady state thermal resistance of the wall assembly was determined following the procedure outlined in ASTM C1363 (ASTM, 2013) for an exterior (cold) side air temperature set point of -35°C and an interior (warm) side air temperature set point of 21°C for both exterior temperatures. The guarded hot box was characterized to determine the combined metering box and flanking losses according to ASTM C1363, to ensure that the measured heat transfer rate was that being transferred through the specimen.

The combined heat transfer coefficients are considered the combined effects due to radiation and convection between the specimen surfaces and the chambers on each side of the specimen. These values were calculated based on the heat flow through the wall assembly and a representative surface temperature. For the interior the average temperature at the centre of the stud cavity was used, and for the exterior the average surface temperature was used. Results for the heat transfer coefficients and measured ambient air temperatures on each side of the specimen during the GHB test are presented in Table 1. The combined heat transfer coefficients and ambient temperature are used as boundary conditions for numerical heat transfer modeling in future work.

Table 1: Total heat transfer coefficient calculation results

	Combined Heat Transfer Coefficient [W/m²K]	Ambient air Temperature [°C]
Interior	6.6	20.9
Exterior	8.4	-34.9

Wall assembly description and instrumentation locations

The wall assembly evaluated for this test sequence measured 2.44 m (96in.) in height, 2.44 m (96 in.) in width, and 197 mm (7.75 in.) in depth. The wall assembly consisted of: an interior gypsum board sheathing, measuring 15.875 mm (0.625 in.) thick; 6 mil Vapour barrier sealed with curtainwall/acoustical caulking at steel studs; 1.09 mm thick (18 gauge) steel studs 92 mm (3.625 in.) in depth, 32 mm (1.25 in.) in width, spaced 406mm (16 in.) on centre; mineral fibre cavity insulation, 88.9 mm (3.50 in.) in depth, press-fit into the cavity between the studs in depth; XPS-VIP-XPS sandwich panels, consisting of an interior XPS sheet at 12.7mm (0.5 in.) thick, a VIP at 25 mm (1 in.) thick, and an exterior XPS sheet at 50.8 mm (2 in.) thick, held in place by fibreglass Z-Bar attached to the steel stud frame. The XPS was sealed at all joints with caulking. Fasteners consisted of #8 self-tapping flat head screws spaced at 203 mm (8 in.) on centre around the perimeter, and spaced 305 mm (12 in.) on centre along the height of interior studs. The materials and dimensions used in the wall assembly are listed in Table 2 and a sketch of the layers of the wall assembly is shown in Figure 1.

As mentioned previously, the composition of the VIP barrier film is not made available on the manufacturer website. Contacting the manufacturer resulted in the following description of the barrier film composition and core material. The barrier film is a tri-layer aluminized film with a total thickness of 97 microns (0.097mm) consisting of three layers of aluminized olyester and a single layer of linear low density polyethylene for heat sealing. The core material is made up of opacified silica consisting of pyrogenic silica and a silicon carbide based opacifier with reinforcing fibers made of glass, polyester or cellulose. There are not getters in the core material.

Table 2: Summary of wall assembly materials and dimensions.

Layer	Description
1	15.875 mm (5/8 in.) Gypsum board
2	6 mil (0.254 mm) polyethylene vapour barrier
3	Mineral fibre insulation (89mm, 3.50 in.)
4	18 gauge (1.09 mm) thick Steel Stud, with fiberglass clips for mounting VIP sandwich panels, spaced at 400mm on centre
5	XPS-VIP-XPS sandwich panel layer (from interior to exterior) – 12.7mm (1/2 in.) XPS, 25mm (1 in.) VIP panel, 50mm (2 in.) XPS.

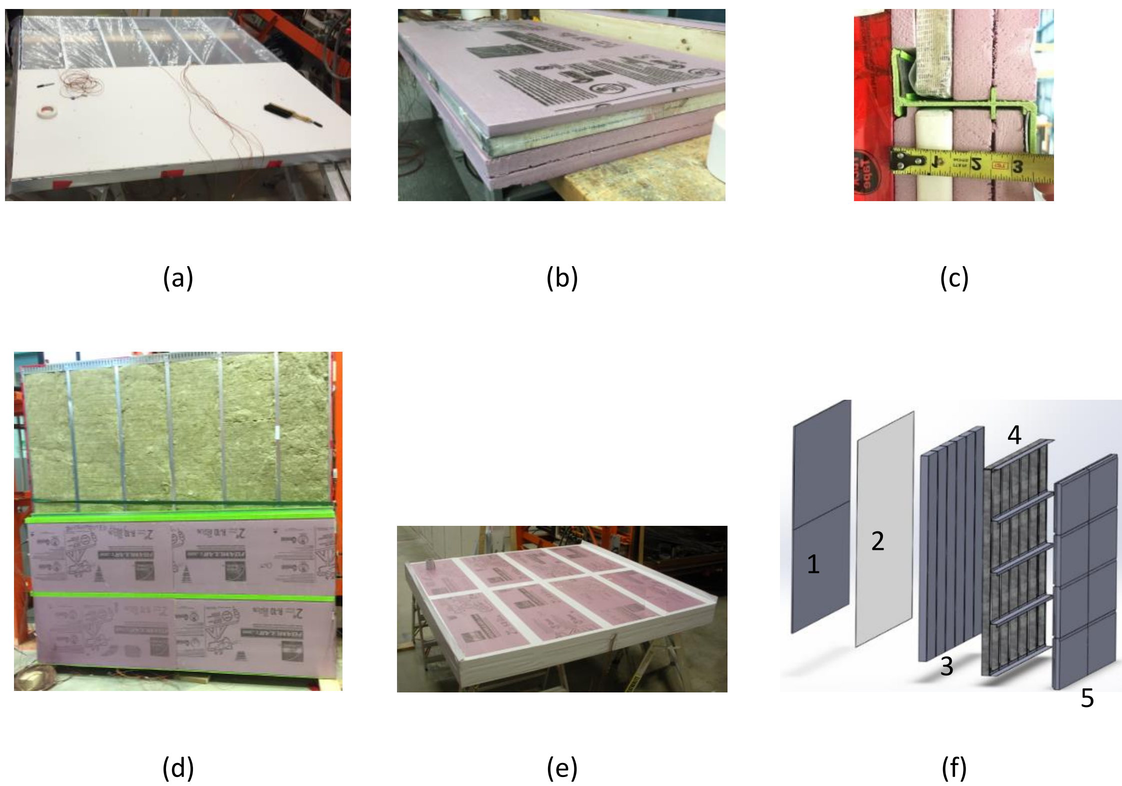

Figure 1: Schematic of wall assembly layers. (a) shows the gypsum layer being installed over the steel studs and the vapour barrier; (b) shows a representative XPS-VIP-XPS sandwich panel; (c) shows a representative fiberglass clip (dimension in inches on tape measure); (d) photo showing mineral fibre insulation and sandwich panel install; (e) shows the complete wall assembly with 8 distinct XPS-VIP-XPS sandwich panels installed; and, (f) shows the wall assembly layers, wherein numbers are from Table 6.

In Figure 1, layer 5 represents the XPS-VIP-XPS sandwich layer, which were made by adhering XPS to the interior and exterior side of 600mm x 1200mm x 25mm VIP panels. The XPS layers were added to the VIP panel to protect the VIP surface from coming in to contact with sharp or abrasive surfaces in the wall assembly, including the surface and edges of the steel studs, the fiberglass clips holding the panels in place, and the fasteners from the exterior strapping. There were eight (8) sandwich panels installed in the wall assembly.

The XPS panels were slightly oversized (>600mm high, >1200mm wide) in each sandwich assembly compared to the VIP dimensions to ensure that adjacent VIP edges would not be in contact in the wall assembly' a representative panel edge is shown in Figure 2.

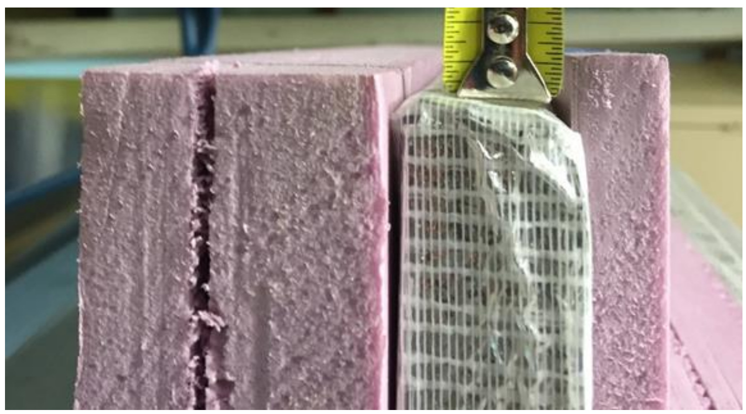

Figure 2: Close up photo of the XPS-VIP-XPS sandwich panel demonstrating the slightly oversized XPS panels (The tape measure is in inches).

Due to construction tolerances and the oversized XPS portions of the sandwich assembly, the butt jointed panels resulted in slight air gaps. To eliminate the effect of the vertical air gap between XPS panels, caulking was added to the vertical joints. Air gaps at the vertical VIP panel joint in the centre of the wall assembly and between the VIP and the fiberglass clips were not filled. All seams were sealed on the exterior surface with tape to ensure that air exchange did not occur between these air joints and the exterior environment during testing. In addition, the air leakage of the wall assembly was tested in a separate apparatus previous to the GHB test, which resulted in an air leakage of the wall assembly of 0.033 L/s-m^2 at a pressure difference of 75Pa. The air leakage tests were completed following the procedures in ASTM E2178 (ASTM E2178-13, 2013) adapted for a full scale wall.

Representative photos of the butt joint, air gaps present in the assembly and the final taped exterior surface are shown in Figure 3.

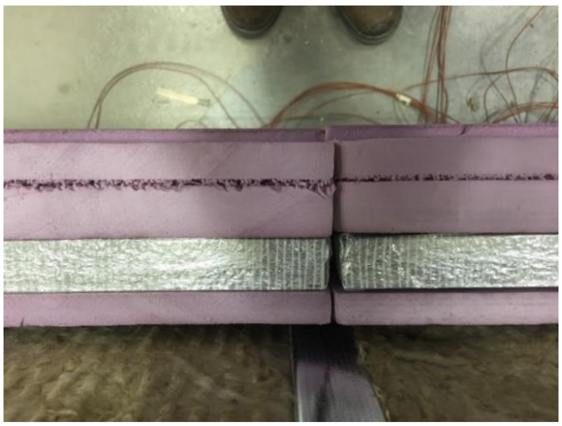

(a)

(b)

(c)

Figure 3: Photos depicting the assembly air gaps that existed between XPS-VIP-XPS at the air joint between VIP panels (a); the air joint at the fiberglass clips (b) (the tape measure is in inches); and the taped exterior surface to eliminate air exchange with the cold exterior (c).

The air gaps at the vertical joints horizontal joints between the VIP panels the VIP Panel and the fiberglass clips were measured and average values are presented in the representative cross section drawings shown in Figure 4 .

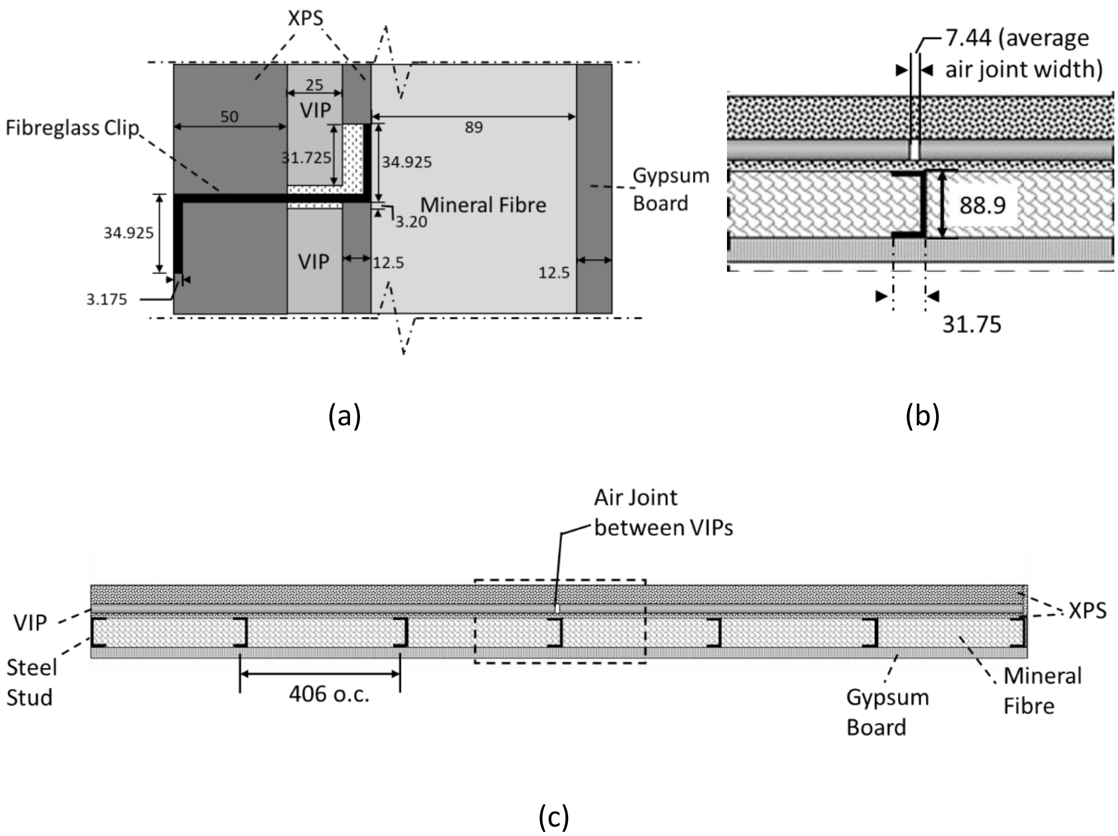

Figure 4: Representative top and side view cross sections depicting the dimensions of the horizontal gaps surrounding the fiberglass clips, all dimensions are in millimetres. (a) Depicts the horizontal air gaps surrounding the clip at each layer; (b) Depicts a zoom in around the stud and centre VIP gap; (c) shows a topview with each stud location and material labelled.

Material properties

The material properties of each component as per reference values or manufacturer advertised values is provide in Table 3. The table also includes the mean temperature at which the materials were characterized. These values reflect the generic material properties that would be available to building designers and engineers for calculations in compliance to energy code requirements. For the VIP, given the variability in effect of the heat transfer at the barrier film edge on the effective thermal conductivity for different film compositions and VIP sizes, it would have been desirable to measure the exact thermal performance of the VIPs used in the GHB test. However, given the size of the VIPs (1200mm wide by 600mm high) this was not possible in the available heat flow meter or guarded hot plate apparatus.

Table 3: Material properties

Material	Reference	Effective thermal conductivity [W/mK]
XPS	ASHRAE Handbook of Fundamentals (T_{mean} = 24°C)	0.029
Steel stud	ASHRAE Handbook of Fundamentals (T_{mean} = 24°C)	48.0
Mineral fibre	Manufacturer (T_{mean} = 24°C)	0.036
Gypsum	ASHRAE Handbook of Fundamentals (T_{mean} = 24°C)	0.16
VIP	Manufacturer centre of panel value (T_{mean} = 10°C)	0.0042
	Manufacturer design value (stated to include barrier film edge effect and service life effects) (T_{mean} = 10°C)	0.0061

Instrumentation

Temperature measurements were made using Type T thermocouples to determine the air temperatures, wall surface temperatures and the temperature of several areas of interest in the wall assembly. The thermocouples were adhered to the surfaces of the wall assembly with two layers of tape. The first layer of tape was aluminum duct tape used to ensure that the thermocouple tip was held in precise contact with the surface it was measuring. The thermocouple was adhered to the wall using the aluminum tape for at least 100mm (4 in.) of its length to avoid the thermocouple adversely affecting the temperature at the location of measurement at the tip junction. The aluminum sheathing tape was covered by a second layer of white masking tape to shield the taped area from radiation effects.

The interior surface of the wall assembly was instrumented to account for surface temperature variations with 20 thermocouples. The thermocouples were arranged to account for variations in surface temperature between the centre of stud cavity and steel stud thermal bridge locations. The thermocouple instrumentation pattern is shown in Figure 5. The exterior surface was instrumented in the directly opposite of the interior surface such that thermocouples lined up through the wall assembly.

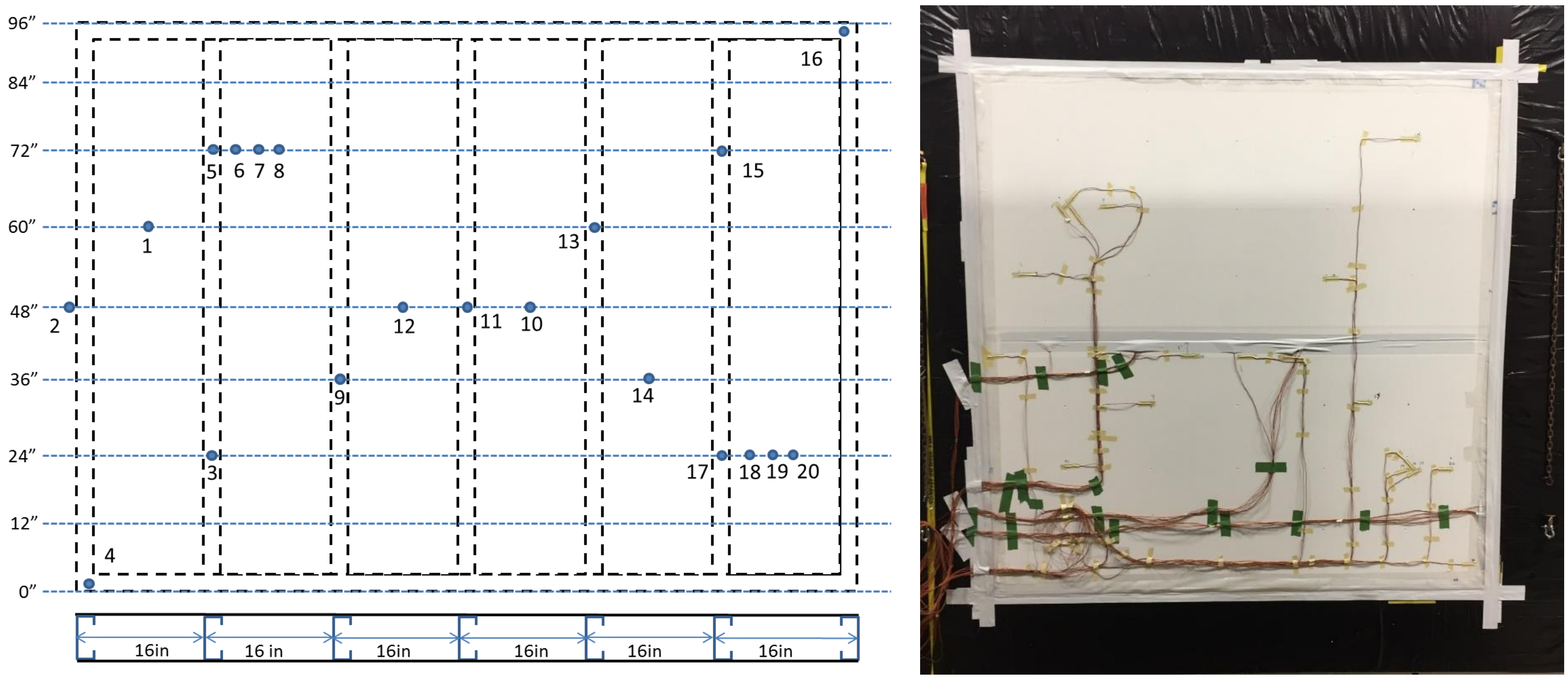

286

Figure 5: Interior surface thermocouple instrumentation map.

The surface thermocouples were installed to determine the effect of the steel stud on the interior temperature. The thermocouple locations on the surface by thermocouple number from Figure 5 are given in Table 4. It is estimated that the thermocouples were installed within ±5 mm (~0.20 in) of the nominal location.

Table 4: Surface thermocouple locations

Thermocouple location	Thermocouple label
Centre of stud cavity (single)	1, 10, 12, 14
Centre of steel stud flange (single)	3, 9, 11, 13, 15
Centre of steel stud flange	5, 17
1 in. (25mm) from centre steel stud flange	6, 18
2 in. (50 mm) from centre steel stud flange	7, 19
8 in. (200 mm) from centre steel stud flange/centre cavity	8, 20
Corner	4, 16
Edge	2

In addition to the thermocouples on the surface of the wall assembly, several other areas of interest within the wall assembly were instrumented with thermocouples. The areas of interest in the wall assembly were from interior to exterior in the mineral fibre insulation at the centre of the stud cavities and the temperature distribution from the centre to the edge of the VIP interior and exterior surfaces. For the purposes of this paper, only the effect of the steel stud on the interior sheathing board temperature and the centre to edge temperature variation in the VIPs are presented.

Centre to edge temperature distribution on VIP surface

The interior and exterior surfaces of a single VIP were instrumented to determine the difference in temperature between the centre of the panel and edge of panel during the test. The thermocouple locations for the VIP panel are shown in Figure 6.

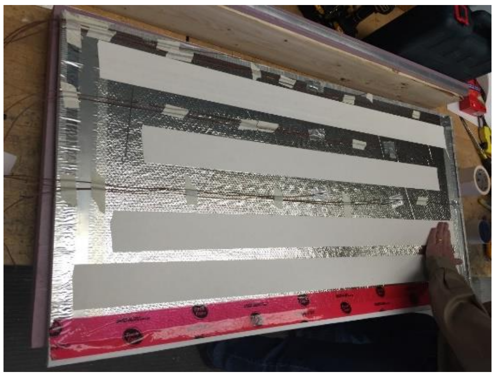

(a)

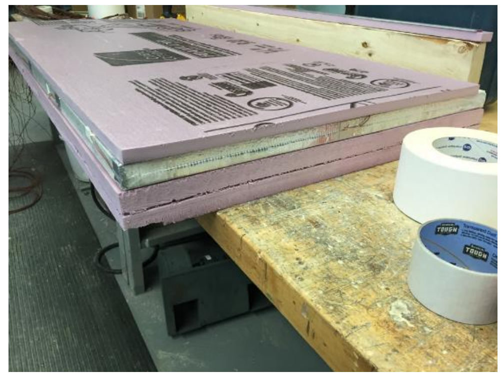

(b)

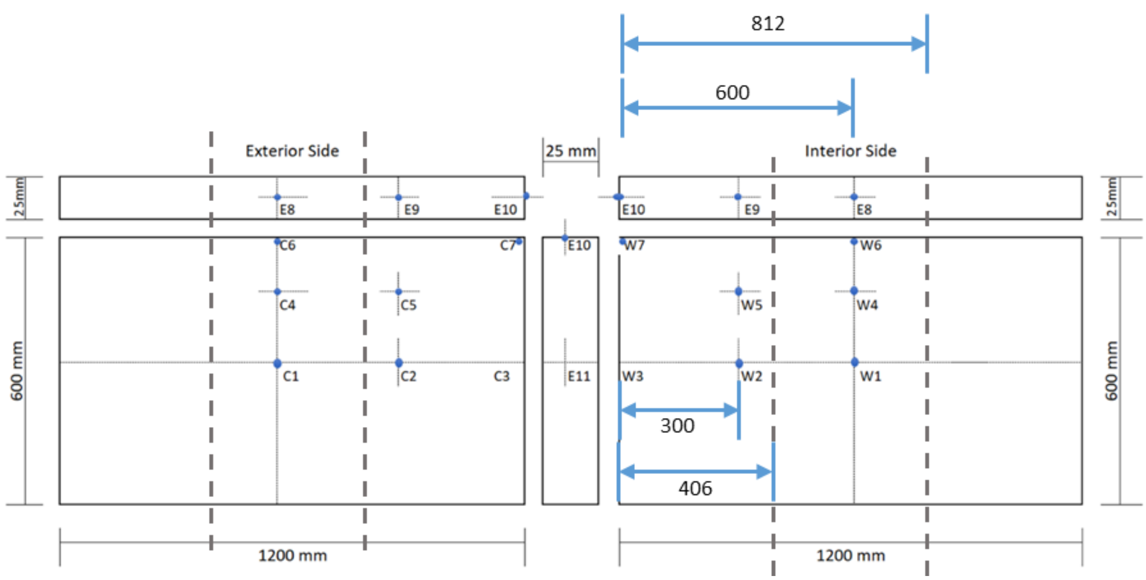

(c)

Figure 6: The top left photo depicts the thermocouples instrumented on the VIP on the exterior (cold) surface of the VIP (a). The top right photo depicts the sandwich panel assembly and shows the edge thermocouples (b). The bottom photo is a graphical representation of the location of all thermocouples installed on the interior (warm, 'W') surface, exterior (cold, 'C') surface, and edge ('E') of the VIP (c); the dashed grey lines represent where the steel studs are located in proximity to the temperature sensors.

In the VIP panels there are three over length seams from the barrier foil. These occur along one long edge, and along the two short edges. These seams are folded around the edge of the VIP, and sealed to the middle of the panel and the panel was oriented such that the seams faced the warm side of wall assembly. As can be seen in Figure 7 there are three warm side thermocouples located on the seams: W6, W7 and W3.

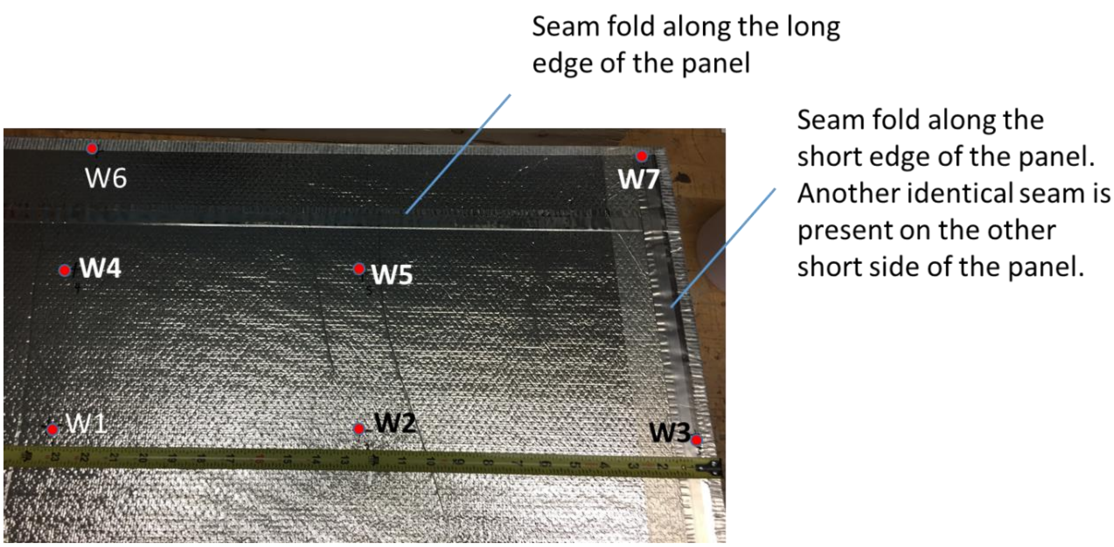

Figure 7: Picture denoting location of sealed seams and thermocouple (red dots) placement.

Experiment uncertainty

The uncertainty of the GHB test results was determined for the temperature measurements and the thermal resistance calculation. The temperature measurement uncertainty was determined as the combined thermocouple uncertainty (root sum square) including the uncertainty of the thermocouple material, uncertainty of the cold junction reference temperature and the uncertainty of the data acquisition. The thermal resistance uncertainty was determined using the method as described by Moffat (Moffat, 1988) accounting for a 95% confidence interval ($1.96*\sigma$). The thermal resistance uncertainty included the combined uncertainty of: the thermocouples, heat input to the metering box (resistive heater measurement of voltage and current), the specimen area (estimated based on tape measure), metering box heat transfer to the guard room (from metering box calibration procedure and thermopile uncertainty), and flanking loss through the specimen guard (estimated based on uncertainty in calibrated specimen properties). The metering box and flanking losses characterization was completed on a homogenous specimen made of XPS, for which the temperature dependent thermal conductivity was determined using a heat flow meter.

The combined thermocouple uncertainty was determined as ±0.45°C, and the combined uncertainty in the thermal resistance of the GHB test was ±11.7%.

Experiment results

As discussed, the steady state thermal resistance of the wall assembly was characterized for a weather side air temperature of -34.9°C with a metering box air temperature of 20.9°C. The experiment results of the "air to air" thermal resistance calculation is presented in Table 5. The "air to air" thermal resistance includes both the thermal resistance of the wall assembly, and the thermal resistance of the air film coefficient on each side of the wall.

Table 5: Thermal resistance calculation results.

R value (RSI, m^2K/W)	6.8 ± 0.8
R value ($hrft^2°F/Btu$)	39 ± 4.54

For context, a simplistic calculation was performed using the parallel path method and the material properties presented in Table 3. Typically, the modified zone method (Kosny, 1995) should be used when performing calculations with steel studs, however the insulation value of the XPS-VIP-XPS would require extrapolating the zone factor beyond the chart available in the ASHRAE Handbook of Fundamentals (ASHRAE, 2016). Using the centre of panel value for the thermal conductivity results in an air to air thermal resistance estimate of 11.1 m^2K/W and 9.2 m^2K/W. Clearly these are significant overestimates of the thermal resistance of the wall assembly and indicate that more complex calculations, or more accurate material properties are needed.

Effect of steel stud thermal bridge on gypsum surface temperature

The interior surface of the gypsum sheathing board was instrumented to determine the effect of the steel stud thermal bridge on surface temperature. The surface temperature of the interior sheathing board is an important performance factor for several reasons, including: that differences in temperature on the surface relate to the amount of heat being transferred through the sheathing board, that colder sections can be at risk to condensation, and that the surface temperature relates to how comfortable a room feels to human occupants.

The effect of the steel stud thermal bridge on the interior surface temperature of the gypsum was measured using thermocouples adhered to the gypsum surface. The thermocouples were installed in a horizontal line, extending away from the centre of the steel stud flange steel stud towards the centre of the stud cavity. The interior surface temperature at points 17 to 20 extending from the steel stud to the centre of the cavity in proximity to the steel stud results is shown in Figure 8. The grey dotted line represents the steel stud location in relation to the surface thermocouples (the steel stud is interior to the surface however).

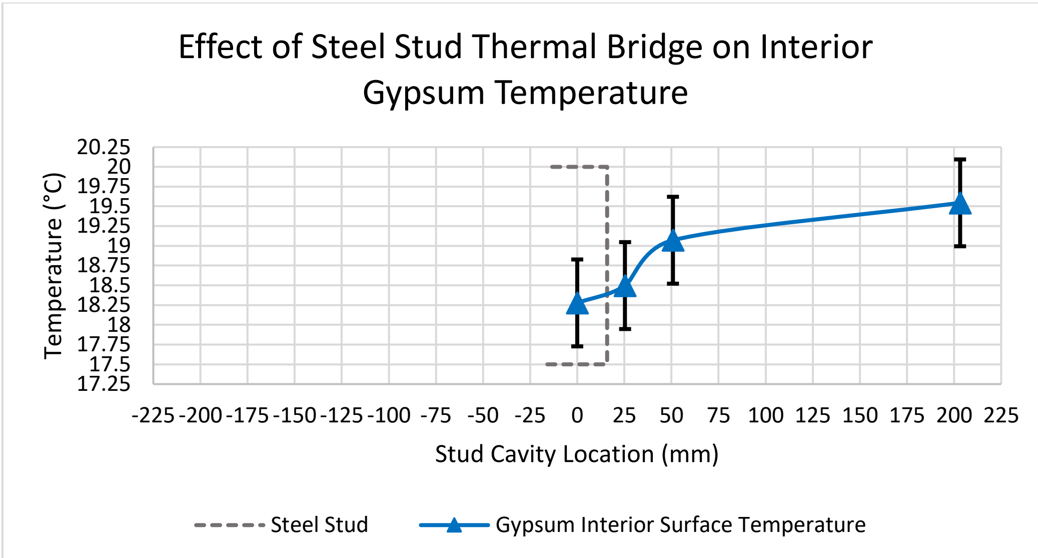

(a)

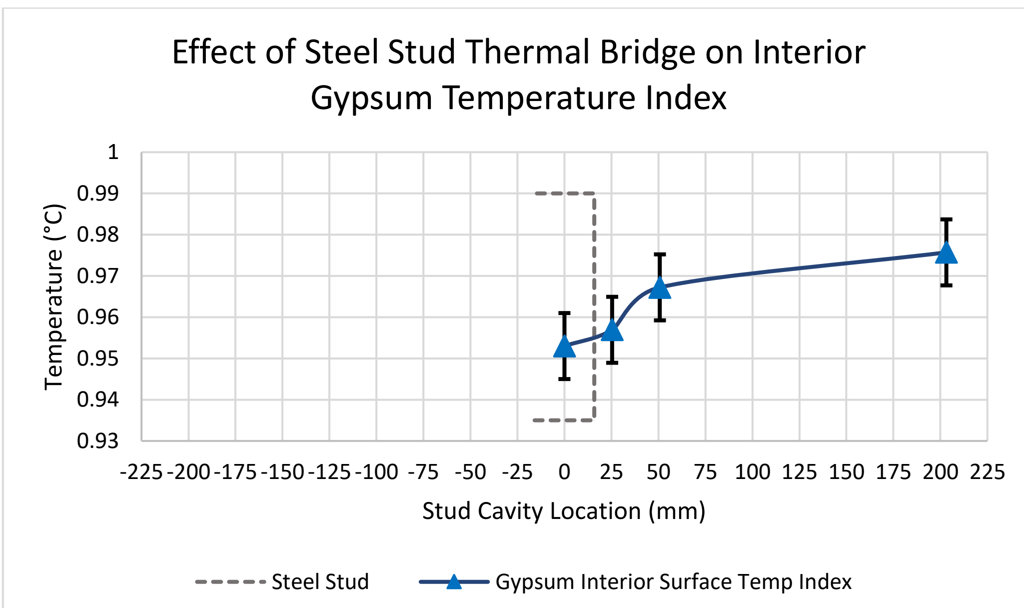

(b)

Figure 8: Interior gypsum surface temperature (a) and surface temperature index (b) for thermocouples 17 to 20.

The results show that the thermal bridge effective area is larger than the physical contact area between the stud and the gypsum board. This effect is well documented for thermal bridges (ASHRAE, 2011) (Kosny,

1995) (Morris and Hershfield, 2014) (Doran & Gorgolewski, 2002). This effect is of note in highly insulated walls, as thermal bridges can be the most significant contributors to heat transfer.

In addition to heat transfer effects, it is important to consider the effect of thermal bridges on the surface temperature of the gypsum to assess the condensation risk of the wall assembly (ASHRAE, 2016) (Morris and Hershfield Ltd., 2011) (National Research Council Canada, 2015). Although the effect of the steel stud thermal bridge is evident on the surface temperature in this wall assembly (and correspondingly the thermal resistance), the potential for localized condensation at the steel stud contact area is low, as the dew point temperature for conditions of 21°C and 55% RH is 11.6°C (at 21°C the interior humidity would have to be higher than 84% to have condensation issues at the stud location). Therefore, in this wall assembly, while the steel stud effects the interior surface temperature of the gypsum, it does not cause a condensation risk to the interior sheathing board.

VIP temperature distribution

A representative VIP panel was instrumented on the interior and exterior surfaces to determine the temperature variation from centre of the panel to the edges. The results for each exterior temperature location from Figure 6 is shown in Table 6.

Table 6: Interior and exterior VIP surface temperature for exterior temperatures of -35°C. The thermocouples are labelled for interior side (W), exterior side (C) and edge (E), numbers as per Figure 6.

	-35°C		-35°C		-35°C
W1	-2.5	**C1**	-19.2	**E8**	-13.3
W2	0	**C2**	-17.8	**E9**	-12.2
W3	-4.6	**C3**	-14.9	**E10**	-3.6
W4	-3.7	**C4**	-19.2	**E11**	-4.2
W5	-7.0	**C5**	-18.2		
W6	-1.6	**C6**	-17.9		
W7	-5.5	**C7**	-13.7		

The results presented in Table 6 generally indicate that a higher rate of heat transfer is occurring through the edges than through the centre of the panel. For the exterior (cold, C) surfaces, this trend is evident with the temperature in the centre being the coldest and getting warmer towards the edges.

Analyzing the results shows that the centre of panel value has a temperature of -19.2 (C1), which increases to -14.9 (C3), -13.7 (C7) and -17.9 (C6) at the edges. The intermediate temperatures measured at C2, C4 and C5 also indicate a warming trend compared to the centre of panel value, with C4 measuring the same as the centre of panel temperature.

The interior (warm, W) surface shows less consistent trends. The centre of panel value for the -35°C temperatures exhibit a centre of panel temperature of -2.5°C (W1), and edge temperatures of -4.6°C (W3), -5.5°C (W7) and -1.6°C (W6). The temperatures measured at W3 and W7 follow the trend; however, W6 is warmer than W1, which would indicate less heat transfer is occurring at that edge than the centre of panel. The intermediate values are also inconsistent with W4 and W5 being colder than the center panel value, while W2 is warmer.

Two reasons that the results could show inconsistent trends is that the presence of the steel studs on the interior side of the panel, or that the thermocouples are not bonded to the panels in close enough contact. However, without the ability to check these conditions directly it is not possible to determine what directly causes these discrepancies. Additionally, the thermocouple wires have been run from edge to centre, due to data acquisition position requirements during test, which could also lead to discrepancies.

Although the interior is not as consistent as the exterior surface in demonstrating the increased heat transfer at the edge versus the centre of the panel, there is still evidence for this phenomena in most centre to edge comparisons. The inability to further resolve the effect of the steel stud on the interior temperature increases the uncertainty of the interior trends. Using the more consistent exterior side, the effect of the edge is clearly exhibited and experimentally demonstrates that designing wall assemblies with VIP's without accounting for edge and joint heat transfer is likely to lead to underestimations in heat transfer rate calculations

Conclusions

This paper determined the thermal resistance of a highly-insulated wall containing both steel studs and VIPs, for which the composition of the barrier film is unknown, through a guarded hot box (GHB) test. A detailed description of the wall assembly construction and an estimate of the uncertainty in the test results was also included. The wall was instrumented to determine the effect of the steel stud thermal bridge on the interior surface temperature and the temperature difference between the centre and edge of a VIP. The tests were completed in accordance with ASTM C1363 for an exterior air temperature of -34.9°C, and an interior air temperature of 20.9°C. The resulting air to air thermal resistance was determined as 6.8 ± 0.8 m^2K/W.

Instrumentation on the exterior side of a VIP demonstrated that more heat transfer occurred at the edges of the panel than through the centre of the panel. The interior side of the panel had less consistent results, but still generally demonstrated increased rates of heat transfer at the edges of the panel compared to the centre values. This is consistent with literature findings for VIPs, and indicates that calculation methods that use the centre of panel value for thermal transmittance calculations are likely overestimating the performance of the wall assembly.

Instrumentation on the interior of the gypsum panel demonstrated that the presence of steel studs in the wall assembly caused a temperature decrease of approximately 1.2°C for the gypsum surface temperature when compared to the centre of stud cavity (i.e. away from the influence of the steel stud) gypsum surface temperature. This demonstrates that the exterior insulation sandwich panel sufficiently insulates the steel studs such that condensation issues are unlikely; the relative humidity would have to be greater than 84% at 21°C for condensation to occur.

The results from these GHB tests can be used by designers and engineers who are considering the use of a similar wall assembly configuration to indicate the potential for compliance to energy and building code requirements. Future work will use the results of this GHB test to explore industry standard calculation methods and two and three-dimensional heat transfer simulations to predict the total thermal transmittance (and correspondingly the thermal resistance) of this wall assembly. This comparison can be used to indicate the potential for use of the calculation and simulation methods in lieu of testing for a wall assembly containing VIPs and steel studs.

Acknowledgments/Declarations

This work was completed with the support of the National Research Council of Canada; however this institution did not have influence in study design; in the collection, analysis and interpretation of data; in the writing of the report; nor in the decision to submit the article for publication.

References

ASHRAE. (2011). *RP-1365 Thermal Performance of Building Envelope Details for Mid- And High-Rise Buildings.* ASHRAE.

ASHRAE. (2016). *ANSI/ASHRAE/IES Standard 90.1-2019 -- Energy Standard for Buildings Except Low-Rise Residential Buildings.* Atlanta, GA: ASHRAE.

ASHRAE. (2016). *ASHRAE Handbook of Fundamentals.* Atlanta, GA: ASHRAE.

ASTM. (2013). ASTM C 1363 - Thermal Performance for Building Materials and Envelope Assemblies by means of a Hot Box apparatus. *ASTM Standards*.

ASTM. (2015). ASTM C518 - Standard Test Method for Steady-State Thermal Transmission Properties by Means of the Heat Flow Meter Apparatus.

ASTM E2178-13. (2013). *ASTM E2178-13 - Standard Test Method for Air Permeance of Building Materials.* West Conshohocken PA: ASTM International.

Atsonios, I., Mandilaras, I., Kontogeorges, D., & Founti, M. (2018). Two methods for the in-situ measurement of the overall thermal transmittance of cold frame lgihtweight steel-framed walls. *Energy and Buildings*, 183-194.

Atsonios, I., Mandilaras, I., Manolitsis, A., Kontogeorgos, D., & Founti, M. (2007). Experimental and Numerical investigation of the Energy Efficiency of a Lightweight Steel Framed building incorporating Vacuum Insulation Panels. *6th International Energy in Buildings Conference*.

Biswas, K., Desjairlais, A., Smith, D., Letts, J., Yao, J., & Jiang, T. (2018). Development and tehrmal performance verification of composite insulation boards containing foam encapsulated vacuum insulation panels. *Applied Energy 228*, 1159-1172.

Brunner, S., Stahl, T., & Wakili, K. G. (2012). Single and double layered vacuum insualtion panels of the same thickness comparison. *Building Enclosure Science Technology Conference (BEST3).* Atlanta.

Doran, S., & Gorgolewski, M. (2002). *U-values for light steel frame construction (Digest 465).* BRE.

Ghazi Wakili, K., & Nussbaumer, T. B. (2005). Thermal Performance of VIP assemblies in Building Constructions. *7th Itnernational Vacuum Insulation Symposium*, 131-138.

Ghazi Wakili, K., Bundi, R., & Binder, B. (2004). Effective thermal conductivity of vacuum insulation panels. *Building Research and Information*, 293-299. doi:10.1080/0961321042000188644

Government of Canada. (2018). *Pan-Canadian Framework on Clean Growth and Climate Change.* Ottawa, Canada: Government of Canada.

ISO 10211-07. (2007). *Thermal bridges in building constructions - Heat flows and surface temepratures - Detailed Calculations.* Geneva, CH: ISO.

ISO 14683-07. (2007). *Thermal bridges in building construction - Linear thermal transmittance - Simplified methods and default values.* Geneva, CH: ISO.

ISO 6946-07. (2007). *Building components and building elements -- Thermal resistance and thermal transmittance -- Calculation method.* Geneva, CH: Internation Organization for Standardization.

Kontogeorgos, D., Atsonios, I., & Mandilaras, I. F. (2016). Numerical investigation of the effect of vacuum insulation panels ont eh thermal bridges of a lightweight drywall envelope. *Journal of Facade Design and Engineering 4*, 3-18.

Kosny, J. (1995, July). Comparison of Thermal Performance of Wood Stud and Metal Frame Wall Systems. *Thermal Insulation and Budiling Environments, 19*.

Lorenzati, A., Fantucci, S., Capozzoli, A., & Perino, M. (2014). The effect of different materials joint in vacuum insulation panels. *6th International Conference on Sustainability in energy and Buidlings*, (pp. 374-381).

Mandilaras, I., Atsonios, I., Zannis, G., & Founti, M. (2014). Thermal performance of a building envelope incorporating ETICS with vacuum insulation panels and EPS. *Energy and Buildings 85*, 654-665.

Moffat, R. (1988). Describing the Uncertainties in Experimental Results. *Experimental and Thermal Science*, 1:3-17.

Morris and Hershfield. (2014). *Building Envelope Thermal Bridging Guide.*

Morris and Hershfield Ltd. (2011). *Thermal Performance of Envelope Details for Mid- and High-Rise Buildings(1365-RP).* Vancouver, B.C., Canada: Morris and Hershfield Ltd.

National Research Council Canada. (2015). National Building Code.

National Research Council Canada. (2016). *National Energy Code for Buildings Canada.* Ottawa, ON: National Research Council Canada.

Nussbaumer, T., Bundi, R. T., & Muehlebach, H. (2005). Thermal analysis of a wooden door system with integrated vacuum insulation panel. *Energy and Buildings 37*, 1107-1113.

Nussbaumer, T., Ghazi Wakili, K., & Tanner, C. (2006). Experimental and numerical investigation of thermal perfromance of a protected vacuum-insulation system applied to a concrete wall. *Applied Energy 83*, 841-845.

Schwab, H., Stark, C., Wachtel, J., Ebert, H.-P., & Fricke, J. (2005). Thermal Bridges in Vacuum-insulated Building Facades. *Journal of Thermal Env. and Bldg. Sci.*, 345-355.

Simmler, H., Brunner, S., Heinemann, U., Schwab, H., Kumaran, K., Mukhopadyaya, P., . . . Stramm, C. T. (2005). *Vacuum Insulation Panels - Study on VIP Components and PAnels for service Life Prediction in Building Applications (Subtask A).* International energy agency. Switzerland: EMPA.

Sprengard, C., & Holm, A. (2014). Numerical examination of thermal bridging effects at the edges of vacuum insulation panels (VIP) in various constructions. *Energy and Buildings 85*, 638-643.

Tenperik, M., & Cauberg, H. (2007). Effects Caused by Thin High Barrier Envelopes around Vacuum Insulation Panels. *Journal of Building Physics*.

United Nations. (2015). *Paris Agreement.* Geneva, CH: United Nations.

Van Den Bossche, N., Moens, J., Janssens, A., & Delvoye, E. (2010). *Thermal Performance of VIP panels: Assessment of the edge effect by experimental and numerical analysis.* Ghent: Ghent University, Department of Architecture and Urban Planning.